CrossMark

PHYSIOLOGICAL ECOLOGY - ORIGINAL RESEARCH

The role of isohydric and anisohydric species in determining ecosystem-scale response to severe drought

D. T. Roman[1] · K. A. Novick[1] · E. R. Brzostek[2] · D. Dragoni[3] · F. Rahman[4] · R. P. Phillips[5]

Abstract Ongoing shifts in the species composition of Eastern US forests necessitate the development of frameworks to explore how species-specific water-use strategies influence ecosystem-scale carbon (C) cycling during drought. Here, we develop a diagnostic framework to classify plant drought-response strategies along a continuum of isohydric to anisohydric regulation of leaf water potential (Ψ_L). The framework is applied to a 3-year record of weekly leaf-level gas exchange and Ψ measurements collected in the Morgan-Monroe State Forest (Indiana, USA), where continuous observations of the net ecosystem exchange of CO_2 (NEE) have been ongoing since 1999. A severe drought that occurred in the middle of the study period reduced the absolute magnitude of NEE by 55 %, though species-specific responses to drought conditions varied. Oak species were characterized by anisohydric regulation of Ψ_L that promoted static gas exchange throughout the study period. In contrast, Ψ_L of the other canopy dominant species was more isohydric, which limited gas exchange during the drought. Ecosystem-scale estimates of NEE and gross ecosystem productivity derived by upscaling the leaf-level data agreed well with tower-based observations, and highlight how the fraction of isohydric and anisohydric species in forests can mediate net ecosystem C balance.

Keywords Carbon flux · Water regulation · Eddy covariance · Stomatal conductance · Net ecosystem exchange

Communicated by David R. Bowling.

✉ K. A. Novick
knovick@indiana.edu

1 School of Public and Environmental Affairs, Indiana University-Bloomington, 702 North Walnut Grove Avenue, Bloomington, IN 47405, USA

2 Department of Biology, West Virginia University, 53 Campus Drive, Morgantown, WV 26505, USA

3 Department of Geography, Indiana University-Bloomington, 702 North Walnut Grove Avenue, Bloomington, IN 47405, USA

4 Department of Biology, The University of Texas Rio Grande Valley, 1201 West University Drive, Edinburg, TX 78539, USA

5 Department of Biology, Indiana University-Bloomington, 1001 East Third Street, Bloomington, IN 47405, USA

Introduction

The composition and functioning of Eastern US forests reflect ongoing species demographic changes, as well as ecosystem and species-specific responses to climate change. Over the past 200 years, forest composition in the Eastern US has been highly dynamic owing to a remarkable legacy of disturbance. From the mid-nineteenth to early twentieth century, timber harvesting produced dramatic reductions in forest cover (Abrams 2003; McEwan et al. 2011), and in the early twentieth century, the gradual abandonment of agricultural fields increased forest cover in most parts of the region (Shifley 2012; Wear and Greis 2012). This reforestation period was marked by other shifts in the disturbance regime, including the "Smokey Bear" era of fire suppression (Abrams 2003; Nowacki and Abrams 2008; Flatley et al. 2013). Consequently, the species composition of modern-era deciduous hardwood forests

🖄 Springer

contains less of the shade-intolerant and fire-dependent oak species, and more shade-tolerant, mesophytic species like red and sugar maple (*Acer rubrum* and *Acer saccharum*) (Abrams 2003).

Over this same time period, the region has also experienced shifts in the climate regime. Increases in the frequency and/or severity of drought events have already been observed in parts of the Eastern US (Ford et al. 2011; Laseter et al. 2012), and are predicted to continue into the future for most temperate regions (Huntington 2006; O'Gorman and Schneider 2009). A number of ecosystem processes, including CO_2 sequestration, wood production, and utilization of water resources, depend directly on the rate of tree C metabolism, which in turn is closely coupled to tree water status. Thus, understanding species-specific adaptive strategies to cope with greater water limitation is critical for understanding ecosystem-scale processes in areas like the Eastern US that are characterized by dynamic species composition and climate regimes.

Recent years have seen a renewed focus and further development on the approach of classifying plant water use, whereby species-specific water-use strategies during periods of hydrologic stress are classified as falling on a spectrum of isohydric to anisohydric behavior (Choat et al. 2012; Manzoni et al. 2013; Klein 2014; Martinez-Vilalta et al. 2014). Isohydric trees regulate stomatal conductance (g_s) to maintain minimum water potential (Ψ) within a relatively narrow range, and thereby reduce the risk of damaging xylem cavitation driven by excessive tension in the trees' hydraulic system (Tyree and Sperry 1988; Choat et al. 2012; Manzoni et al. 2013). However, a consequence of this strategy is that these trees close their stomata in response to even mild water stress—a process which reduces leaf carbon (C) uptake. In contrast, anisohydric trees allow their leaf Ψ (Ψ_L) to decrease during drought by sustaining relatively high g_s (and thus C assimilation); but this strategy incurs a greater risk of cavitation in the xylem, which could ultimately lead to rapid declines in leaf water supply that may affect a range of physiological variables, including photosynthetic capacity and g_s (Tyree and Sperry 1988; McDowell et al. 2008). Anisohydric species will be more susceptible to xylem risk if the midday Ψ achieved by these species are close to the point at which rapid embolism occurs, representing a low safety margin (Choat et al. 2012). We note that low Ψ alone does not indicate a high risk of hydraulic failure if the safety margin is still wide (Plaut et al. 2012).

Much of the existing literature relevant to the isohydric-anisohydric framework relies on observations collected during experimental drought manipulations (Plaut et al. 2012; Meinzer et al. 2014), laboratory-based observations on excised shoots and leaves (Taneda and Sperry 2008; Choat et al. 2012; Martinez-Vilalta et al. 2014), or

modeling exercises (Manzoni et al. 2013). Some studies investigating isohydric/anisohydric behavior in trees experiencing a naturally occurring drought exist (Quero et al. 2011; Thomsen et al. 2013), but few have supported the suite of leaf- and stand-scale observations necessary to determine the role of anisohydric and isohydric species in determining drought impacts on ecosystem-scale C cycling.

Here, we explore the species-specific contributions to stand-scale C dynamics during a severe drought event by leveraging a novel data set of long-term (1999–2013) eddy covariance record of ecosystem-scale C fluxes with a 3-year (2011–2013) data set of weekly leaf-level gas exchange and Ψ_L observations (~8000 leaf measurements). We conducted this research at the Morgan-Monroe State Forest (MMSF) in central Indiana, which received only 23 mm of rainfall during the peak of the 2012 growing season (i.e., June and July), which is less than 10 % of the long-term (1999–2011) mean rainfall in June and July (=242 mm). Further, this drought resulted in the lowest June rainfall amount recorded at a nearby National Weather Service station (KBMG, Bloomington, IN) since the 1933 onset of the Dust Bowl. To our knowledge, these data represent one of the most comprehensive records of leaf- and canopy-scale processes in a mature forest collected in situ during a severe drought event.

The first overarching objective of this study was to determine the relative degree of isohydry/anisohydry in the functioning of common Eastern US tree species during this severe drought event. The second objective was to quantify how these plant water-use strategies affect species-specific patterns in C assimilation and productivity before, during and immediately after the severe drought event. Finally, we place these results in the context of ongoing, management-driven changes in regional forest species composition to assess how shifts from forests dominated by anisohydric to those dominated by isohydric trees may affect ecosystem C balance during future drought events. Our work is focused on two competing hypotheses:

Hypothesis 1 C assimilation will be most limited during the severe drought in isohydric trees, as stomatal closure to regulate Ψ_L will lead to direct reductions in photosynthesis.

Hypothesis 2 C assimilation will be most limited during the severe drought in anisohydric trees, as low Ψ_L could lead to hydraulic system damage that limits water supply to the leaf and impacts the ability to effectively assimilate C.

We stress that these predictions apply to patterns of C assimilation and allocation during and shortly after a single drought event. Over longer time periods characterized by persistently limiting hydrologic conditions, processes

like C starvation and the associated cascade of physiological impacts could become more important (McDowell et al. 2008).

Materials and methods

Study site

The MMSF is a managed deciduous broadleaf forest in south-central Indiana, USA. The average age and height of the trees are 80–90 years and 27 m, respectively. Since 1998, a 46-m AmeriFlux tower has been operating continuously at MMSF (Schmid et al. 2000). Based on basal area data, sugar maple (*Acer saccharum*) is the dominant canopy species followed by tulip poplar (*Liriodendron tulipifera*), sassafras (*Sassafras albidum*) and oaks (*Quercus* spp.*),* which together comprise nearly 75 % of all basal area in plots surrounding the tower (Schmid et al. 2000). Soils in the area are mesic Typic Dystrochrepts dominated by the Berks–Weikert complex. The average depth to bedrock is 2.2 m with a minimum of 0.4 m, and the average rooting depth is 0.44 m. Leaf litter data collected in 2013 show that sugar maple, tulip poplar, sassafras, and oak species constitute 38, 11, 4, and 6 % of canopy leaf area index, respectively.

Ancillary meteorological and edaphic data

During the study period, air temperature and relative humidity were measured with a temperature and humidity probe (HMP45c; Vaisala, Helsinki, Finland) and thermohygrometer (VTP37; Meteolabor, Wetzikon, Switzerland) at 46 m, and were used to estimate vapor pressure deficit (*D*). At four different locations in the footprint of the eddy-covariance tower, soil moisture content (θ) in the first 30 cm of the soil was monitored using time domain reflectometer probes (TDR) (CS615 and CS616; Campbell Scientific, Logan, UT) and scaled using gravimetric samples collected weekly at the TDR monitoring locations. The θ data were then averaged, and a site-specific, empirical model developed by Wayson et al. (2006) was used to estimate soil Ψ (Ψ_S) to a depth of 30 cm ($\Psi_{S,0-30}$) from θ. This model has the form $\Psi_S = -a \cdot b^{c\theta^d}$, with $a = 2.61 \times 10^8$, $b = 189$, $c = -2.51$, and $d = 0.14$ (see Wayson et al. 2006 for more details). It was developed using soil moisture retention curves with psychrometric measurements of Ψ_S and gravimetric measurements of soil water content (Hanson et al. 1998). Soil moisture at depth (>30 cm) was measured using an Envirosmart soil water content probe (Sentek Technologies, Stepney, Australia) beginning in April 2006, and was used to derive a weighted Ψ_S down to 50 cm ($\Psi_{S,0-50}$) by scaling the robust shallow measurements by the relative differences observed at deeper depths. This allowed us to characterize the soil water availability across a wider portion of the rooting zone.

Eddy covariance measurements

Carbon dioxide and water vapor fluxes were measured at the top of the tower (i.e., $z = 46$ m) using a sonic anemometer (CSAT-3; Campbell Scientific) and a closed-path infrared gas analyzer (LI-7000; LI-COR, Lincoln, NE), which is calibrated weekly. Eddy covariance data were recorded continuously at a frequency of 10 Hz and post-processed into hourly fluxes of the net ecosystem exchange of CO_2 (NEE) as described in detail in Dragoni et al. (2011) and Schmid et al. (2000). To fill hourly NEE time series gaps and to partition NEE into ecosystem respiration (RE) and gross ecosystem productivity (GEP), simple parametric models linking soil temperature to RE, and photosynthetic photon flux density to GEP, were applied to the NEE record as described in Dragoni et al. (2011), such that NEE = GEP − RE.

Leaf-level gas exchange and Ψ data

Measurements of midday leaf-level assimilation (*A*) and g_s were recorded each week during the growing seasons of 2011–2013 using a portable photosynthesis system (Li-6400XT; LI-COR) and a 25-m boom lift to access the top of the canopy. Measurements were made on sugar maple [$n = 3$; diameter at breast height (DBH) = 44.2 ± 0.6 cm], tulip poplar ($n = 3$; DBH = 69.8 ± 12.3 cm), and sassafras ($n = 3$; DBH = 36.5 ± 3.6 cm), white oak ($n = 2$; DBH = 38.4 ± 4.6 cm), and red oak ($n = 1$; DBH = 46.3 cm). Each tree was sampled by selecting five leaves at the top of the canopy exposed to direct solar radiation and five leaves in the sub-canopy of the tree (lower half of the canopy). Thus, for each sampling week during the study, 12 trees × 5 leaves × 2 canopy positions = 120 leaves were sampled resulting in ~8000 individual leaf measurements from the 64 sampling weeks of the study period. Chamber photosynthetic photon flux density, CO_2 and water vapor concentrations were set to match ambient conditions in the field. Each measurement was made over a relatively short time period (~2 min) to avoid excessive increases in chamber humidity, which was monitored together with temperature. We aggregated data to species-level averages for canopy and sub-canopy conditions on each measurement day.

We measured Ψ_L concurrent with the gas-exchange measurements using a Scholander-type pressure system (PMS Instruments, Corvallis, OR). One leaf from each tree canopy was covered with aluminum foil for 15 min to allow the Ψ of the leaf cells and the xylem to reach equilibrium,

and to prevent biases related to leaf excision (Turner and Long 1980; Leach et al. 1982). Then, dinitrogen gas was applied to the chamber until water appeared on the cut petiole of the leaf. The pressure required to liberate the water from the non-transpiring leaf is equal in magnitude but opposite in sign to Ψ_L. This process was repeated on one leaf from the sub-canopy of each tree.

Biomass measurements

Leaf area was calculated from litterfall collected using sixteen 0.5-m^2 litter baskets located in the footprint of the tower. To estimate species-specific contributions to leaf area index, litterfall was collected on a bi-weekly interval during the 2013 growing season and was dried, sorted by species, weighed and scanned for leaf area. Every 2 weeks during the growing seasons of 2012 and 2013, we measured the change in the DBH of the sample trees using dendrometer bands. Annual wood production (g C tree^{-1}) was then estimated using published allometric equations and site-specific wood C content (Ehman et al. 2002). Root mass with depth was determined in the summer of 2000 by digging 1-m^2 soil pits to either 1-m depth or to bedrock (whichever came first). This process was repeated in 15 plots within the footprint of the tower. Root samples were collected for varying depths and were then dried, sorted into size classes, and weighed.

Diagnosing isohydric as compared to anisohydric behavior

We adopted two independent approaches for diagnosing isohydric as compared to anisohydric behavior in our study species. The first relies on observed time series of Ψ_S and Ψ_L, which are related to the flux of water from soil to the leaf (J_S) via (Whitehead et al. 1984):

$$J_S = K(\Psi_S - \Psi_L) = K(\Delta\Psi) \tag{1}$$

assuming that K is the whole plant hydraulic conductance, and neglecting the contribution of gravitational head losses to $\Delta\Psi$, which are relatively constant over weekly to monthly timescales. Following the recent synthesis of Martinez-Vilalta et al. (2014), the rate of change in Ψ_L relative to Ψ_S during a drought event (i.e., $\partial\Psi_L/\partial\Psi_S$) tends to be close to zero in the case of isohydric species (Fig. 1a, triangles), and close to or even greater than 1 for more anisohydric species (Fig. 1a, squares). Here, we derive species-specific $\partial\Psi_L/\partial\Psi_S$ from the weekly Ψ_L measurements and the concurrent estimates of $\Psi_{s,0-50}$ inferred from the soil moisture time series. Note that in our analysis, we report slope values ($\partial x/\partial\Psi_s$, where x represents Ψ_L, A or g_s) as positive but show them as negative in figures, which results from the use of $-\Psi_{s,0-50}$ so that movement from left to

right represents a shift from wet to dry conditions (Fig. 1a), consistent with changes in D (Fig. 1c).

A second, novel approach to diagnosing isohydric versus anisohydric behavior relies on the observations of g_s, and thus is less sensitive to biases associated with the Ψ measurements. Under steady-state conditions characterized by negligible boundary-layer resistance and little hydraulic capacitance, J_S may be equated to the leaf-level transpiration rate (T_r), which may be further linked to g_s via $J_S = T_r = g_s D$ (Oren et al. 1999). Thus, a relationship between g_s, D, K, and $\Delta\Psi$ can be obtained:

$$g_s = \frac{1}{D}K(\Delta\Psi) \tag{2}$$

With this relationship, we predict how three idealized scenarios for the evolution of $\Delta\Psi$ during a drought event affect the observed g_s:

Case 1 Perfectly isohydric response: $\partial\Psi_L/\partial\Psi_s = 0$, and the quantity $\Delta\Psi$ decreases over the course of the drying event, reducing g_s and its sensitivity to D relative to wet conditions (Fig. 1c, triangles).

Case 2 Constant $\Delta\Psi$ regulation: $\partial\Psi_L/\partial\Psi_s = 1$, and the quantity $\Delta\Psi$ remains constant. Thus, $g_s \sim 1/D$ for the duration of the drought event (Fig. 1c, solid line).

Case 3 Anisohydric response: $\partial\Psi_L/\partial\Psi_s > 1$, such that quantity $\Delta\Psi$ increases with time, thereby increasing g_s and its sensitivity to D (Fig. 1c, squares).

For cases 2 and 3, the hydraulic conductivity may also decrease over the course of a dry-down event as increasingly large tensions in the plant's hydraulic pathways promote xylem embolism (Sperry 2000). If the decrease in K is greater than the increase in $\Delta\Psi$, then g_s and its sensitivity to D will decrease in a manner analogous to the isohydric case (i.e., case 1). It is important to note that utility of Eq. 2 is principally diagnostic. While the form of Eq. 2 implies a direct dependence of g_s on $\Delta\Psi$, in actuality it is plant regulation of g_s that determines $\Delta\Psi$. Further, this approach relies on the assumption of no hydraulic capacitance, which would be invalidated if the trees rely on stored water during the day (Phillips et al. 2003; Meinzer et al. 2009).

To quantify how the functional relationship between g_s and D changes over the course of the drought, gas-exchange data were extracted that met conditions defined in one of the following three classifications: (a) wet conditions, when $\Psi_{S,0-30}$ was greater than the minimum Ψ_S typically observed during non-drought periods (= -0.5 MPa); (b) drought conditions when $\Psi_{S,0-30} \leq -0.5$ MPa, including dry periods of 2011 and 2012; and (c) post-drought-conditions,

Fig. 1 Theoretical expectations for the behavior of isohydric versus anisohydric species over the course of a prototypical dry-down event. **a** Relationship between leaf water potential (Ψ_L) and soil Ψ (Ψ_S) expected for isohydric behavior (*Case 1*), anisohydric behavior (*Case 3*) and an intermediate case (*Case 2*). **b** How leaf-level assimilation (*A*) relative to wet conditions relates to Ψ_S for isohydric (*triangles*) and anisohydric (*squares*) plants, with *grey lines* showing the anisohydric case with 50 and 90 % loss of hydraulic conductance (*K*) occurring by the end of the dry-down. **c** How the relationship between stomatal conductance (g_S) and vapor pressure deficit (*D*) is expected to change as a reflection of isohydric regulation (*triangles*), anisohydric behavior (*squares*), or the intermediate case (*solid line*) with changes in *K* and $\Delta\Psi$, which represents the difference between Ψ_S and Ψ_L. **d** How the relative reductions in *A* translate to ecosystem-scale reductions in gross primary productivity (*GPP*) as the fraction of isohydric species in the canopy varies from 0 to 1, where in these simulations, the balance of species were assumed to be anisohydric plants experiencing a range of *K* sensitivity


occurring from mid-August [day of year (DOY) 220] to late September (DOY 273) of 2012. Within each class, species-specific functions of the form:

$$g_s = a - bD^{-1/2} \tag{3}$$

were fit from linear regression of all available point measurements of conductance and chamber *D*. While Eq. 2 relates g_s to $1/D$, the more flexible form of the model of Eq. 3, which also has theoretical support (Katul et al. 2009), better incorporates the mechanisms by which variations in *K* and $\Delta\Psi$ can mediate the dependence of g_s on *D* (e.g., Fig. 1c); 90 % confidence intervals on the predicted g_s for each species in each class were generated using a bootstrap approach with 1000 iterations.

Linking leaf-level *A* to isohydric/anisohydric behavior

In the case of constant water-use efficiency, isohydric regulation of Ψ_L promotes a negative relationship between *A* and Ψ_S over the course of the dry-down event (triangles, Fig. 1b), whereas anisohydric regulation of Ψ_L can lead to relatively constant *A* over the course of a dry-down event if the losses in *K* are minimal (Fig. 1b, squares). However, if losses in *K* are large, then the sensitivity of *A* to hydrologic limitation can be comparable to, or greater than, that associated with an isohydric plant (Fig. 1b, grey lines). If the trends in Fig. 1b are representative of whole plant behavior, then the fractional reduction to total GEP can be estimated for a range of hypothetical species compositions representing a gradient of 100 % isohydric species to 100 % anisohydric species (Fig. 1d). When losses in *K* are minimal, the GEP of a canopy dominated by isohydric species will be more significantly reduced during a drought event (Fig. 1d, black line; hypothesis 1). However, if losses to *K* are large, then the relative reduction in GEP will be greater in a stand dominated by anisohydric species (Fig. 1d, light-grey line; hypothesis 2).
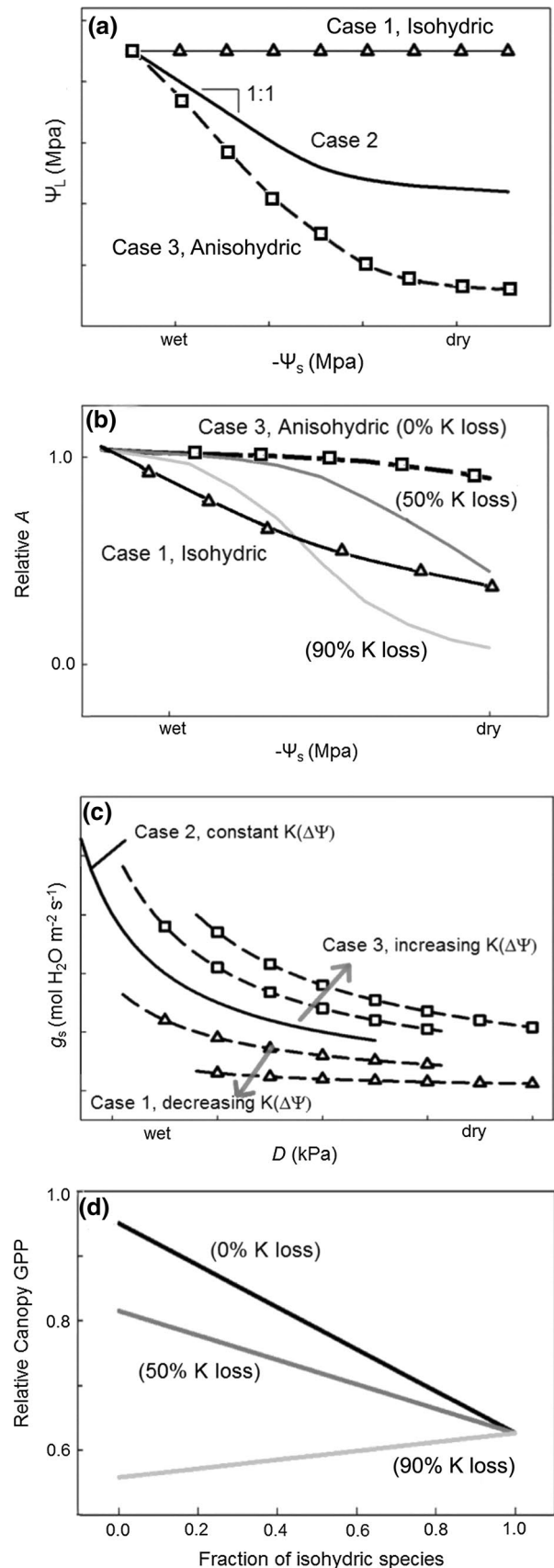
Scaling to canopy GEP

The leaf-level gas exchange rates were scaled to a canopy-scale estimate of GEP using species-specific relationships between A and $\Psi_{S,0-50}$ developed after dividing the data into wet, drought, and post-drought periods as described above. For each of these periods, linear regression analysis was used to evaluate the species-specific relationship between A and $\Psi_{S,0-50}$. For those periods and species with a significant relationship, we then predicted daily midday A using the daily average of $\Psi_{S,0-50}$. If this regression was not significant, then the mean values across the entire period were used. Once daily midday A values were calculated for each species, the ratio of drought (2012) versus non-drought (2013) midday A was determined. This relative reduction in A was then scaled to the ecosystem level (A_{total}) based on the relative fraction of species-specific leaf area.

The scaling approach was assessed by comparing the scaled ratios of 2012:2013 A_{total} to the 2012:2013 ratio of tower-based estimates of GEP during the growing season. After validation, the scaling approach was used to determine the ratio of midday A_{total} in 2012:2013 across a range of hypothetical distributions in the abundance of isohydric versus anisohydric species while maintaining consistent relative contributions from each species (i.e., tulip poplar, which comprises 20 % of the leaf area of isohydric canopy dominants at MMSF, was always ~20 % of the isohydric portion).

The scaling exercise was performed using upper-canopy data. While not a focus of this manuscript, leaf-level gas exchange measurements were performed on sub-canopy leaves as well. As detailed in the supplementary information (Online Resource), the trends in A, g_s, and Ψ_L during the course of the drought event were similar for both canopy levels, particularly when comparing the relative change from wet conditions (Online Resource Figs. 1–6). The sub-canopy data were not explicitly incorporated into the scaling exercise due to a lack of vertical estimates of the distribution of light and species-specific leaf area. Nonetheless, as we show in the online materials, the temporal trends in the relative reductions to upper- and lower canopy gas exchange are statistically similar, and thus the results of our efforts to predict the relative, canopy-averaged declines in photosynthesis during drought as a function of species composition are not particularly sensitive to assumptions about the fraction of sunlit and shaded leaves.

Statistical analyses

Linear regression analysis was used to evaluate the response of A and g_s to the reduction in $\Psi_{S,0-50}$ during the drought of 2012. The analysis was performed primarily with Matlab and SPSS statistical software packages. Each species was tested for significance in their slope and intercept parameters and then these parameters were analyzed for differences between species and between canopy and sub-canopy data using a two-tailed t-test. Species-specific differences in regulation of plant water status were assessed using a regression analysis for changes in midday Ψ_L with changing $\Psi_{S,0-50}$. Linear relationships were developed over the entire period for midday canopy samples and separately for only 2012 data. Slope parameters were then compared across species with relationships that were significantly different from zero.

Results

Meteorological conditions during the study period

From late 2011 up to and including mid-2012, MMSF experienced a severe drought event that was unique in both timing and magnitude. The initial drying period started in mid-July 2011 and persisted through much of the 2012 growing season with minimum weekly $\Psi_{S,0-30}$ averages of −1.4 and −1.6 MPa in 2011 and 2012, respectively (Fig. 2a). Soil dry-downs near the end of the growing season are typical at MMSF, but this particular drought event was unique in that the soil dried to a $\Psi_{S,0-30}$ of −1.0 MPa by mid-July in 2012 (Fig. 2a), which is 10 weeks earlier than that of the baseline mean (calculated from 1999 to 2010) and 6 weeks earlier than any other year. When considering soil conditions at depth (e.g., $\Psi_{S,0-50}$), the observed trends were similar but the variations were smaller in magnitude as the deeper layers did not experience such a severe decline in soil moisture. Growing season D was also exceptionally high during the drought in 2012 (Fig. 2b). The final year of the study (2013) was characterized by wet conditions in which $\Psi_{S,0-30}$ did not drop below a weekly mean of −0.39 MPa.

Ecosystem C and water fluxes during the study period

At the ecosystem level, the absolute magnitude of NEE was reduced to unprecedented levels during the drought (Fig. 2c). During the peak of the 2012 growing season (DOY 182–218), the absolute value of measured NEE (sum of hourly fluxes for July up to and including mid-August) in 2012 was reduced by 102 g C, or 55 %, relative to baseline (1999–2010) mean NEE (Fig. 2c). GEP and RE were also reduced by the drought (Fig. 2d, e), but during the peak of the growing season, the reductions in GEP relative to the baseline mean (162 g C m^{-2} and 40 %, respectively) exceeded reductions in RE (56 g C m^{-2} and 24 %, respectively), leading to a smaller C sink overall.

Fig. 2 Weekly averages of **a** Ψ_S down to 30 cm ($\Psi_{S,0-30}$), **b** D, **c** net ecosystem exchange of CO_2 (*NEE*), **d** gross ecosystem productivity (*GEP*), and **e** ecosystem respiration (*RE*) in 2011 (*grey dashed line*), 2012 (*black dashed line*), and 2013 (*light-grey solid line*). The *grey shaded area* shows the range of weekly averaged observations for 1999 to 2010, while the *solid black line* represents the average of these years. For other *abbreviations*, see Fig. 1
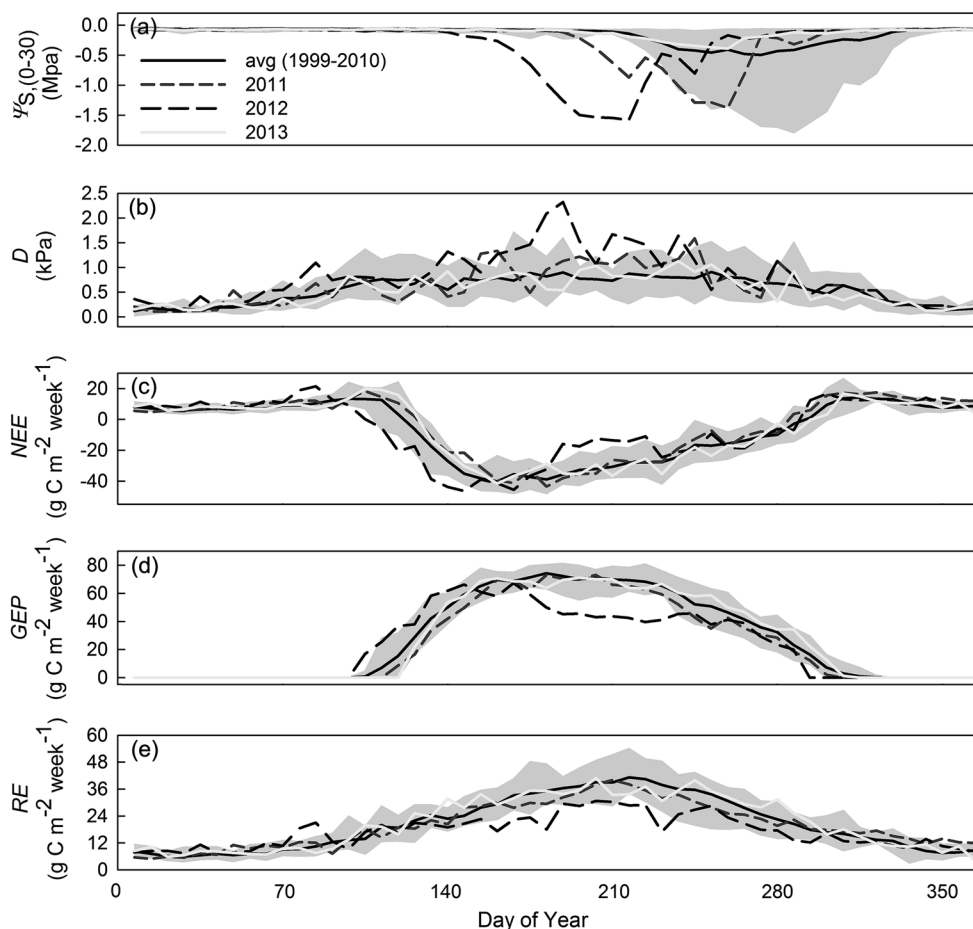
At annual time scales, the NEE for 2012 (-300 g C m^{-2}) was ~88 % of the baseline mean (-348 g C m^{-2}). Similarly, the annual GEP was 83 % of the baseline mean, and the annual RE was 87 % of the baseline mean. The annual GEP and RE in 2012 were the lowest in the site's 15-year history of flux measurements, though smaller annual NEE values were observed in 2009 and 2011.

The annual fluxes in 2012 were strongly affected by an abnormally early start to the growing season. The date at which weekly averaged NEE first crossed zero in 2012 (DOY = 98) occurred about 3 weeks earlier than average (mean DOY = 118 for the period 1999–2010; Fig. 2c). The early growing season led to an additional 81 and 102 g C m^{-2} of NEE and GEP from DOY 0–151, relative to the baseline mean. Factoring out the effects of the early growing season results in estimates of annual NEE and GEP in 2012 that would be 63 and 76 % of the long-term mean, respectively.

Temporal trends in A, g_s, and Ψ_L, and the relationship of these variables to Ψ_S

In general, the A of oak species was greater than the A of sassafras and tulip poplar, which in turn were greater than the A of maple (Fig. 3b). In 2011, A and g_s reached a maximum for all species around DOY 200 (Fig. 3b, c), and then generally decreased during the growing season. During 2012, oaks maintained high A and g_S throughout most of the drought-affected growing season, while significant reductions in gas exchange rates during the drought were observed for the other species (Fig. 3b, c). Large decreases in Ψ_L were observed over the course of the growing season for oak species (Fig. 3a). In the wet growing season of 2013, the magnitudes of A, g_s, and Ψ_L changed little with time and were more similar across species.

The slope of the relationship between $\Psi_{S,0-50}$ and Ψ_L (i.e., $\partial\Psi_L/\partial\Psi_s$; Fig. 4a) was only significant for oaks and tulip poplar when considering data from 2012, with stronger relationships observed for oak species (white oak, $\partial\Psi_L/\partial\Psi_s = 1.31$ MPa MPa^{-1}, $r^2 = 0.79$, $p < 0.001$; red oak, $\partial\Psi_L/\partial\Psi_s = 1.5$ MPa MPa^{-1}, $r^2 = 0.80$, $p < 0.001$) than tulip poplar ($\partial\Psi_L/\partial\Psi_s = 0.30$ MPa MPa^{-1}, $r^2 = 0.15$, $p = 0.05$). The $\partial\Psi_L/\partial\Psi_s$ differed significantly among tulip poplar and both oak species (white oak, $t = -6.94$, $df = 24$, $p < 0.001$; red oak, $t = -8.29$, $df = 24$, $p < 0.001$), but

Fig. 3 Time series of canopy leaf gas exchange and Ψ_L measurements made from 2011 to 2013 shown as daily species averages with SE. Data for *white oaks* (*Quercus alba*) are shown in *dark-grey downward triangles*, red oaks (*Quercus rubra*) in *white triangles*, sugar maple (*Acer saccharum*) in *light-grey squares*, tulip poplar (*Liriodendron tulipifera*) in *grey diamonds* and sassafras (*Sassafras albidum*) in *black circles*. **a** Midday Ψ_L, **b** A measured at ambient conditions, **c** calculated g_s during those periods. For other *abbreviations*, see Fig. 1
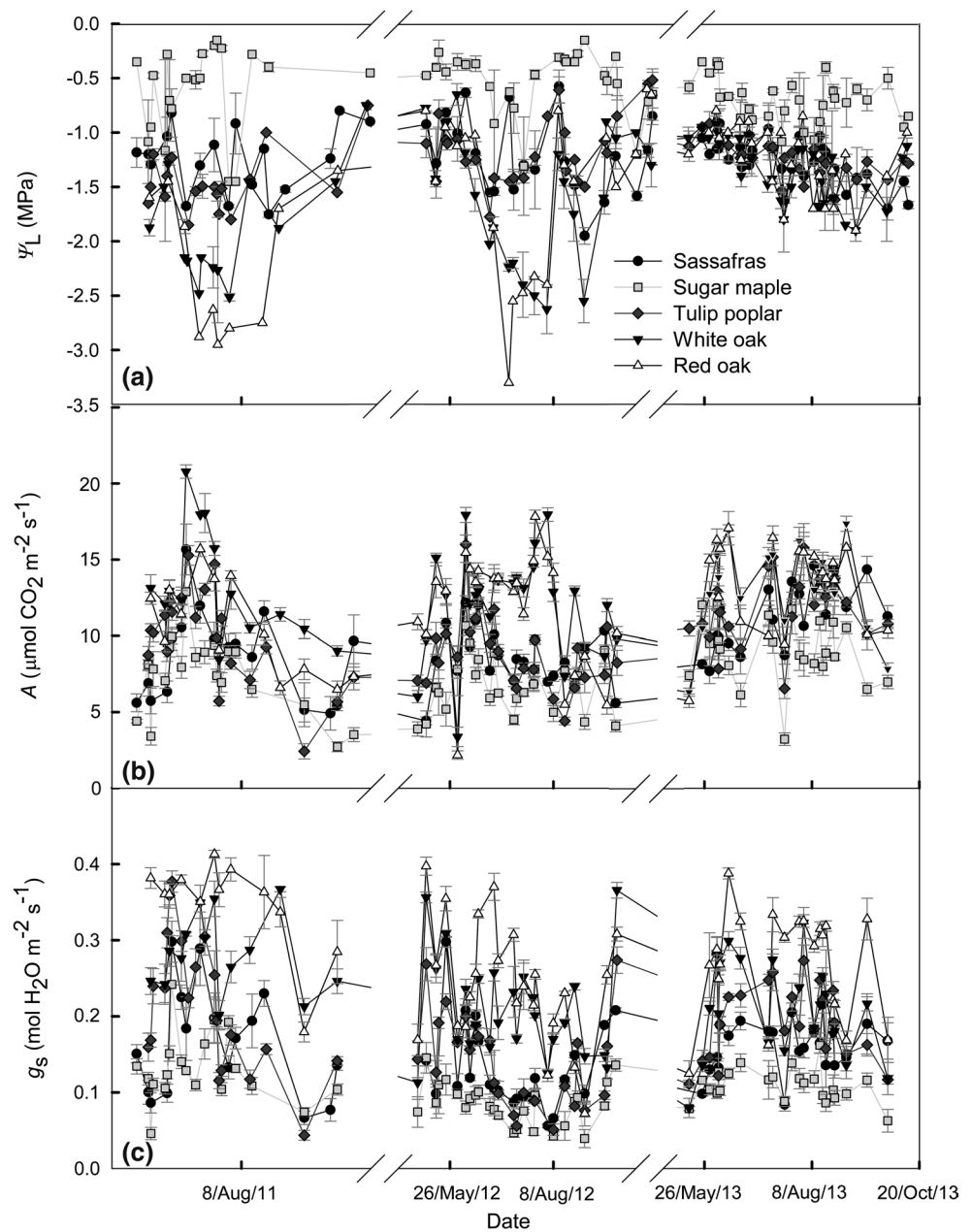
not between oak species ($t = -1.39$, $df = 22$, $p = 0.18$). Similar trends were observed when data from all years were included as well as when analyzing sub-canopy data (Online Resource Fig. 5).

There were significant relationships between $\Psi_{S,0-50}$ and A during the 2012 drought for all study species except white oak (Fig. 4b). A strong reduction in A per unit reduction in $\Psi_{S,0-50}$ was observed for tulip poplar ($\partial A / \partial \Psi_S = 5.9$ μmol CO_2 m^{-2} s^{-1} MPa^{-1}, $r^2 = 0.69$, $p = 0.003$). The slope parameter $\partial A / \partial \Psi_S$ was smaller but still significant for sugar maple and sassafras (sugar maple, $\partial A / \partial \Psi_S = 3.79$ μmol

CO_2 m^{-2} s^{-1} MPa^{-1}, $r^2 = 0.62$, $p = 0.007$; sassafras, $\partial A / \partial \Psi_S = 3.33$ μmol CO_2 m^{-2} s^{-1} MPa^{-1}, $r^2 = 0.57$, $p = 0.012$). The $\partial A / \partial \Psi_S$ associated with red oaks was relatively small ($\partial A / \partial \Psi_S = 2.07$ μmol CO_2 m^{-2} s^{-1} MPa^{-1}, $r^2 = 0.62$, $p = 0.01$). Similarly, g_s declined significantly with declining $\Psi_{S,0-50}$ in all species but oaks (Fig. 4c). The greatest declines in g_s with decreasing $\Psi_{S,0-50}$ were observed for tulip poplar ($\partial g_s / \partial \Psi_S = 0.12$ mol H_2O m^{-2} s^{-1} MPa^{-1}, $r^2 = 0.85$, $p < 0.001$). The slope parameter $\partial g_s / \partial \Psi_S$ was not as great for maple and sassafras (sugar maple, $\partial g_s / \partial \Psi_S = 0.035$ mol H_2O m^{-2} s^{-1} MPa^{-1},

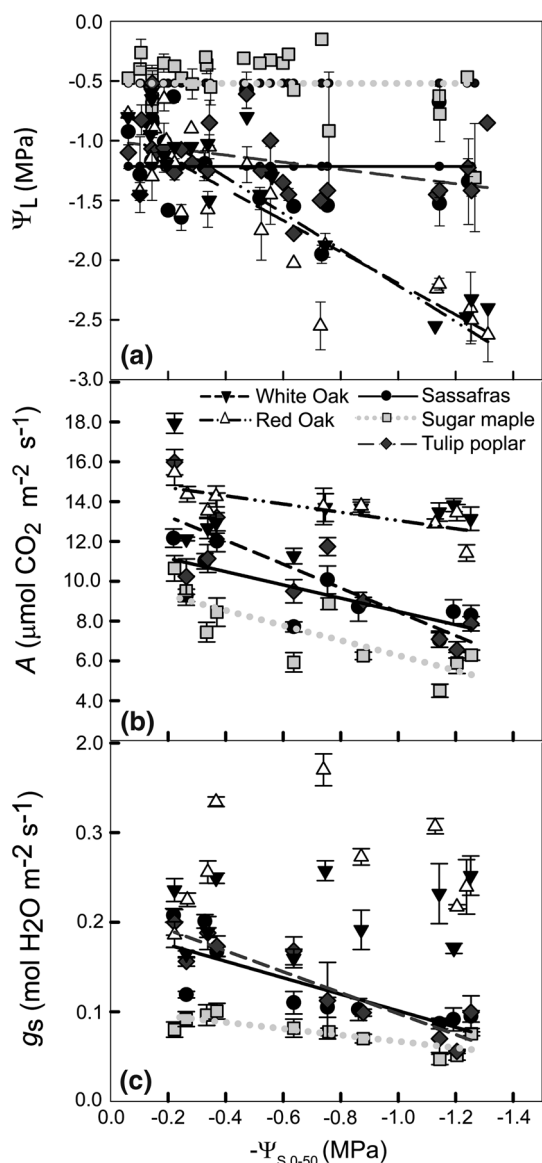**Fig. 4** The relationships between Ψ_L (**a**), A (**b**), and g_s (**c**) with Ψ_s down to 50 cm ($\Psi_{S,0-50}$). Ψ_L are from the entire growing season of 2012 while A and g_s data are from only the drought period of that year. Significant linear relationships between Ψ_L and $\Psi_{S,0-50}$ were observed for tulip poplar (slope = 0.3, $P = 0.05$), white oak (slope = 1.3, $P < 0.001$) and red oak (slope = 1.5, $P < 0.001$), but not for sassafras or sugar maple (*lines* represent mean values). Note that these slopes are reported as positive but appear negative due to the *x*-axis showing $-\Psi_{S,0-50}$. Linear relationships between A with $\Psi_{s,0-50}$ were found for sassafras ($P = 0.01$), sugar maple ($P = 0.007$), tulip poplar ($P = 0.003$) and red oak ($P = 0.01$), while the relationships between g_s with $\Psi_{S,0-50}$ were only found for sassafras ($P = 0.005$), sugar maple ($P = 0.005$) and tulip poplar ($P < 0.001$). For other *abbreviations*, see Figs. 1 and 3

$r^2 = 0.65$, $p = 0.005$; sassafras, $\partial g_s / \partial \Psi_S = 0.082$ mol H_2O m^{-2} s^{-1} MPa^{-1}, $r^2 = 0.65$, $p = 0.005$). These parameters were also computed for the sub-canopy data and show generally similar trends (Online Resource Figs. 1–6).

Temporal variation in the relationship between g_s and D

The relationship between g_s and D (i.e., Eq. 3 parameterized from observations) was similar throughout the study period for sassafras and maple (Fig. 5a, b), but a clear departure in the relationship between g_s and D during the peak of the 2012 drought period was observed for tulip poplar (Fig. 5c) and oak species (Fig. 5d). Relative to wet conditions (Fig. 5, triangles), the magnitude of tulip poplar g_s, and its sensitivity to D, decreased significantly during the drought period (Fig. 5c, grey squares). For example, at a reference $D = 2$ kPa, the g_s of tulip poplar declined from 0.15 mmol m^{-2} s^{-1} during wet conditions to 0.1 mmol m^{-2} s^{-1} during the drought period (Fig. 5c). In contrast, at a reference D of 2 kPa, g_s of oak species increased from 0.205 mmol m^{-2} s^{-1} during wet conditions to 0.235 mmol m^{-2} s^{-1} during the peak of the drought. During the post-drought period (i.e., mid-August up to and including September 2012), the magnitude of g_s was lower than that observed during wet conditions for both tulip poplar and oaks (Fig. 5c, d, circles).

Woody C increment

A trend toward reduced wood C accumulation in 2012 as compared to 2013 was observed in all species (Table 1), though due to a limited sample size the effect was only significant at the 95 % confidence level for tulip poplar, with an average of 76 % less C accumulation in 2012 than 2013 ($df = 2$, $t = -5.496$, $p = 0.032$). This compares with an average reduction of 52 % for sassafras ($p = 0.121$) and 44 % for maple ($p = 0.059$). The oaks were associated with the lowest reduction with an average decrease in wood C increment of just over 30 % ($p = 0.083$).

Scaling

During the drought period, the ratio of midday A_{total} in 2012 to 2013 derived from species-specific relationships between A and Ψ_S was validated by the high correlation with the 2012:2013 ratio of total daily GEP derived from eddy covariance measurements (Fig. 6a; $r^2 = 0.62$, $p = 0.002$). The estimate of A_{total} derived by classifying species as either anisohydric (i.e., oaks) or isohydric (i.e., maples) reveals that, in a hypothetical forest comprising 100 % anisohydric species that functional similarly to the MMSF oaks, the total growing season GEP in a drought year (e.g., 2012) is statistically unchanged from its value in a wet year (e.g., 2013). Conversely, in a hypothetical forest comprising 100 % isohydric species, the GEP in a dry year is 81 % of its value in a wet year (Fig. 6b).
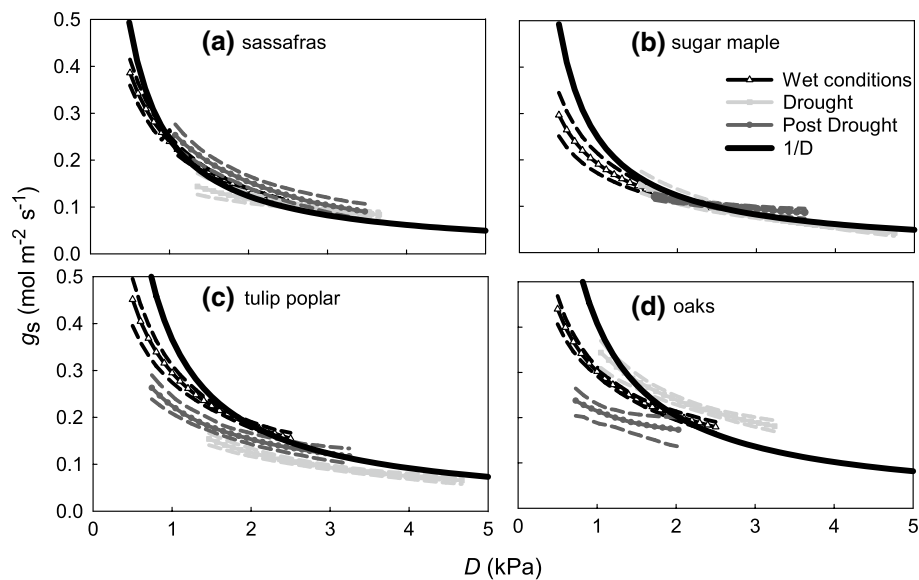
Fig. 5a–d The relationship between g_s and D, as determined by parameterizing the model of Eq. 3 using data from wet conditions (*white triangles* with *black lines*), data from the peak of the drought period (June–July 2012; *light-grey squares* and *lines*), and data from the post-drought period (mid-August to September 2012; *dark-grey circles* and *lines*); 90 % confidence intervals (*dotted lines*) were generated using a bootstrap. For reference, the *thick black line* shows the quantity $1/D$, normalized so that it intersects the wet-condition response at $D = 2$ kPa. This analysis treats observations from the red and white oaks as one collective functional group, as preliminary analysis suggested that the response of g_s to D did not differ significantly among the two species. For *abbreviations*, see Fig. 1

Table 1 Total wood biomass C production during 2012 and 2013 as measured using dendrometer bands and allometric equations

Species	Wood C growth (kg C)		Drought induced % reduction
	2012 (Drought)	2013 (Average)	
Sassafras	3.29	7.23	51.63
Sugar maple	8.19	14.57	43.77
Tulip poplar	4.53	18.96	76.03
Oak (both species)	12.11	16.39	32.76

Data shown are averages of the three individuals of each species and the percent reduction was calculated for each individual and then averaged for each species

Discussion

We leveraged long-term data sets from a deciduous hardwood forest to investigate species- and ecosystem-level C cycling during a drought event that was one of the most severe in the historical record (Mallya et al. 2013; Hoerling et al. 2014; Wang et al. 2014), but nonetheless may be representative of meteorological events that are expected to be more common in the future (Dai 2011). The drought event had significant impacts on GEP, tree growth, and the size of the forest C sink. In particular, the reductions in GEP and NEE (on the order of 55 and 40 %, respectively; Fig. 2) represent climate-change feedbacks which, when they occur over large spatial scales, can accelerate the pace of climate change by reducing the size of the terrestrial CO_2 sink.

The response of GEP to hydrologic limitation depends on the distribution of isohydric and anisohydric species in the forest canopy. Typically anisohydric behavior was observed in the oak trees on the basis of two complimentary approaches. First, Ψ_L decreased more rapidly than Ψ_S among oak species (i.e., $\partial\Psi_L/\partial\Psi_s > 1$; Fig. 4a), consistent with the characterization of anisohydric trees presented by Martinez-Vilalta et al. (2014); second, the magnitude of g_s at a given D, and the sensitivity of g_s to D, increased during the course of the drought for oak species (Fig. 5d), which is consistent with the predictions for anisohydric behavior (Fig. 1c). The drought response of other species was more isohydric, with Ψ_L regulated to a relatively narrow range (i.e., smaller $\partial\Psi_L/\partial\Psi_s$; Fig. 4a). Furthermore, relationships between g_s and D for the non-oak species were more consistent with predictions for isohydric or intermediate behavior (i.e., static or decreasing sensitivity of g_s to D, compare Fig. 1c to Fig. 5a–c).

Trends in the drought response of wood C increment generally followed the observed trends in g_s and A across species, with the smallest reduction observed in oaks and the greatest reduction observed in tulip poplar (Table 1). Importantly, these short-term growth responses to drought appear to mirror decadal responses observed at the MMSF to chronic water stress. A reduction in water availability
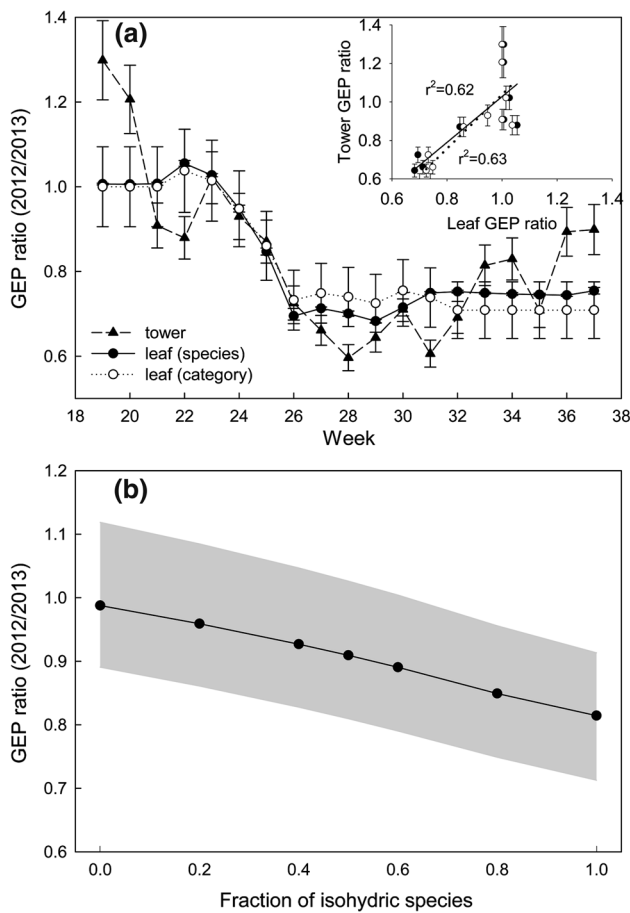
Fig. 6 Results of the scaling exercise. **a** Comparison of the ratio of 2012:2013 GEP (*filled triangles*) and the upscaled analogue (i.e., A_{total}) derived from species-specific relationships (*filled circles*), and the more generic relationships representative of isohydric or aniso-hydric species (*open circles*). *Data points* represent weekly means with *error bars* representing SEM. **a** *Inset* correlation between GEP and A_{total} ratios during the drought period (weeks 19–29). **b** Predicted ratio of 2012:2013 A_{total} for a range of hypothetical species composi-tions reflecting increasing dominance of isohydric species, with the balance comprising anisohydric species. The *shaded area* represents SE as calculated by adjusting daily A values by 1 SE (in slope or mean depending on significance of regression) before scaling to A_{total} using leaf area values. For *abbreviations*, see Figs. 1 and 2

over the decadal scale led to less wood growth in sassa-fras, tulip poplar, and maple, but a very minor reduction observed in oak (Brzostek et al. 2014). Coupled with the work presented here, these results suggest that differ-ences in the leaf-level drought responses of the canopy can impact long-term ecosystem C storage.

These results confirm the predictions of hypothesis 1, and suggest that the large stand-scale reductions in the absolute magnitude of NEE and GEP, and consequently primary productivity, would likely have been larger if it were not for the resilience of the anisohydric oaks to drought. Across varying fractions of isohydric:anisohydric

species, we show that the ratio of total canopy assimilation in a drought year (2012) relative to a wet year (2013) var-ied from 0.81 in the case of a canopy comprising 100 % isohydric species, to 1.0 in the case of a canopy comprising 100 % anisohydric species (Fig. 6b).

The role of hydraulic function in determining species-specific drought response

Oaks have long been recognized to be more drought toler-ant that other deciduous tree species (Abrams 1990; Dick-son and Tomlinson 1996; Meinzer et al. 2013). Nonethe-less, it is surprising that the observed A and g_s of oaks were essentially unchanged over the course of this severe drought event, though such an outcome is not without precedent (Thomsen et al. 2013). Here, we attribute this result to the anisohydric behavior observed in oak species, which we reiterate was confirmed using two complimen-tary but independent approaches. An alternative explana-tion for static gas exchange rates during drought relates to rooting depth, which is often observed to be lower for oaks relative to other species (Abrams 1990) and thus could permit access to deep soil water. Vertical root distri-bution profiles at MMSF reveal that over 85 % of the root biomass is contained within the top 50 cm of the soil (i.e., the depth over which soil moisture was monitored; Online Resource Fig. 7), and previous research at the MMSF has shown that annual wood growth as well as its phenol-ogy is highly correlated with soil water content in the top 30 cm (Brzostek et al. 2014). Nonetheless, we cannot rule out the possibility that oak trees have access to deeper water pools on the basis of existing root biomass meas-urements alone.

Access to deeper water pools during a drought event would minimize reductions in the integrated Ψ_s available to oaks. In the absence of large reductions in K, higher Ψ_s would require a less negative Ψ_L to maintain the same flux of water through the stem (i.e., Eq. 1); however, in these data we observe the opposite response (i.e., more negative Ψ_L for oaks as compared to other species). Furthermore, pre-dawn Ψ_L (data not shown), which are often surrogated by Ψ_S (Ritchie and Hinckley 1975; Richter 1997) was relatively low for oak species (-0.77 ± 0.27 MPa) in the 2012 drought when compared to maples and tulip poplars (-0.16 ± 0.05 and -0.54 ± 0.03, respectively). These data suggest that, on average, the oaks had access to *less* soil water than the other trees; however, this conclusion should be interpreted within the context of processes known to prevent equilibrium between pre-dawn Ψ_L and Ψ_S, includ-ing nocturnal transpiration and refilling of stored water (Bucci et al. 2004).

In summary, the results suggest that for the oak species, the reward of adopting an anisohydric drought response

strategy was worth the risk of reduced water transport capacity, at least with respect to this particular drought event. The relatively low oak g_s observed at the end of the drought period (Fig. 5d) may indicate that some damage to the hydraulic architecture occurred, and our data are not sufficient to assess the extent to which rapid cavitation and refilling of the xylem may have occurred. However, tree-scale estimates of K derived by inverting Eq. 1 were only marginally reduced during the drought period for white oak (Online Resource Fig. 8; slope = -0.016 mmol H_2O m^{-2} s^{-1} MPa^{-1} day^{-1}), and not any other species. These data, and the static g_s rates observed for the oak trees over the course of the drought period (i.e., Fig. 4c), which has also been confirmed with sap flux records of tree water uptake during the study period (data not shown), would suggest that catastrophic xylem failure did not occur. Nonetheless, we recognize that an important area for future research would be to examine how these strategies impact survival during even more severe or prolonged drought events, and whether these strategies impose any lag on C gain in subsequent years due to depletion of C reserves for vascular tissue repair.

Implications for stand-scale C dynamics under future land-use and climate regimes

When interpreted in the context of regional forest dynamics, our results have important implications. Owing to a number of factors, but most notably fire-suppression activities (Nowacki and Abrams 2008), the fractional composition of oaks in eastern deciduous forests, which historically exceeded 50 %, has been declining for decades (Abrams 2003). Our results show that, owing to their anisohydric hydraulic regulation strategy, oaks were more resilient to the severe 2011–2012 drought. The anisohydric tendencies of oak species could be viewed as a factor that may mitigate the pace of oak decline, particularly in a future characterized by increasingly frequent drought events. On the other hand, if the fractional composition of oak continues to decrease, then the results of our scaling exercise predict that the magnitude of the regional C sink could decrease, particularly during drought events, if oaks are replaced with more isohydric species (Fig. 6b). The anisohydric strategy of oaks generally results in more overall water use than isohydric species, which could have major impacts on the hydrological cycle and water resource availability downstream (van der Molen et al. 2011); while these impacts are not the focus of this manuscript, they represent an important area of future research.

The applicability of our mechanistic framework (e.g., Fig. 1) relies on the extent to which plant species may be placed along a continuum of isohydric to anisohydric

hydraulic regulation strategies. One useful metric for quantifying the degree of isohydry is the hydraulic safety margin (Meinzer et al. 2009; Choat et al. 2012; Johnson et al. 2012), which represents the difference between minimum midday stem Ψ and the stem Ψ at which 50 % loss of K occurs ($\Psi_{x,50}$). In the absence of information about the hydraulic safety margin, the $\Psi_{x,50}$ alone may be a useful proxy, as it is directly correlated to the safety margin (see Choat et al. 2012). Among the most common tree species in the Eastern US, a wide range of safety margins and $\Psi_{x,50}$ have been observed (Online resource Table 1). However, oak species are clearly associated with the lowest safety margins and $\Psi_{x,50}$, and thus represent the predominant anisohydric species in Eastern US forests. Among the most isohydric species are the southern pines (*Pinus taeda, Pinus echinata;* Online resource Table 1). The dynamics of southern pine forests at the landscape scale are also highly non-stationary and characterized by a growing fractional cover of southern pine forests to meet growing timber demand for pulpwood (Wear and Greis 2012). The framework of Fig. 1d, when applied at the landscape scale to assess the effect of increasing fraction of isohydric pine forests on regional C dynamics, would suggest a more vulnerable C sink in a future climate regime characterized by great drought frequency/severity, confirming results from recent work (Stoy et al. 2008; Novick et al., in press). In any event, applicability of the framework presented here, and other mechanistic models that link gas exchange to plant hydraulic characteristics, benefits greatly from the growing knowledge base of plant hydraulic characteristics contained in synthesis studies (Meinzer et al. 2009; Choat et al. 2012; Manzoni et al. 2013) and plant-trait data bases (Kattge et al. 2011).

References

Abrams MD (1990) Adaptations and responses to drought in *Quercus* species of North America. Tree Physiol 7(1–4):227–238

Abrams MD (2003) Where has all the white oak gone? Bioscience 53(10):927–939

Brzostek EB, Dragoni D, Schmid HP, Rahman AF, Sims D, Wayson CA, Johnson DJ, Phillips RP (2014) Chronic water stress reduces tree growth and the carbon sink of deciduous hardwood forests. Glob Change Biol 20(8):2531–2539

Bucci SJ, Scholz FG, Goldstein G, Meinzer FC, Hinojosa JA, Hoffmann WA, Franco AC (2004) Processes preventing nocturnal equilibration between leaf and soil water potential in tropical savanna woody species. Tree Physiol 24(10):1119–1127

Choat B, Jansen S, Brodribb TJ, Cochard H, Delzon S, Bhaskar R, Bucci SJ, Feild TS, Gleason SM, Hacke UG et al (2012) Global convergence in the vulnerability of forests to drought. Nature 491(7426):752–755

Dai AG (2011) Characteristics and trends in various forms of the Palmer drought severity index during 1900–2008. J Geophys Res Atmos 116:D12

Dickson RE, Tomlinson PT (1996) Oak growth, development and carbon metabolism in response to water stress. Ann Sci For 53(2–3):181–196

Dragoni D, Schmid HP, Wayson CA, Potter H, Grimmond CSB, Randolph JC (2011) Evidence of increased net ecosystem productivity associated with a longer vegetated season in a deciduous forest in south-central Indiana, USA. Glob Change Biol 17(2):886–897

Ehman JL, Schmid HP, Grimmond CSB, Randolph JC, Hanson PJ, Wayson CA, Cropley FD (2002) An initial intercomparison of micrometeorological and ecological inventory estimates of carbon exchange in a mid-latitude deciduous forest. Glob Change Biol 8(6):575–589

Flatley WT, Lafon CW, Grissino-Mayer HD, LaForest LB (2013) Fire history, related to climate and land use in three southern Appalachian landscapes in the eastern United States. Ecol Appl 23(6):1250–1266

Ford CR, Laseter SH, Swank WT, Vose JM (2011) Can forest management be used to sustain water-based ecosystem services in the face of climate change? Ecol Appl 21(6):2049–2067

Hanson PJ, Todd DE, Huston MA, Joslin JD, Croker J, Augé RM (1998) Description and field performance of the Walker Branch Throughfall Displacement Experiment: 1993–1996, ORNL/TM-13586. Oak Ridge National Laboratory, Oak Ridge

Hoerling M, Eischeid J, Kumar A, Leung R, Mariotti A, Mo K, Schubert S, Seager R (2014) Causes and predictability of the 2012 Great Plains drought. Bull Am Meteorol Soc 95:269–282

Huntington TG (2006) Evidence for intensification of the global water cycle: review and synthesis. J Hydrol 319(1–4):83–95

Johnson DM, McCulloh KA, Woodruff DR, Meinzer FC (2012) Hydraulic safety margins and embolism reversal in stems and leaves: why are conifers and angiosperms so different? Plant Sci 195:48–53

Kattge J, Diaz S, Lavorel S, Prentice C, Leadley P, Bonisch G, Garnier E, Westoby M, Reich PB, Wright IJ et al (2011) TRY—a global database of plant traits. Glob Change Biol 17(9):2905–2935

Katul GG, Palmroth S, Oren R (2009) Leaf stomatal responses to vapour pressure deficit under current and CO_2-enriched atmosphere explained by the economics of gas exchange. Plant Cell Environ 32(8):968–979

Klein T (2014) The variability of stomatal sensitivity to leaf water potential across tree species indicates a continuum between isohydric and anisohydric behaviours. Funct Ecol. doi:10.1111/1365-2435.12289

Laseter SH, Ford CR, Vose JM, Swift LW (2012) Long-term temperature and precipitation trends at the Coweeta Hydrologic Laboratory, Otto, North Carolina, USA. Hydrol Res 43(6):890–901

Leach JE, Woodhead T, Day W (1982) Bias in pressure chamber measurements of leaf water potential. Agric Meteorol 27:257–263

Mallya G, Zhao L, Song XC, Niyogi D, Govindaraju RS (2013) 2012 Midwest drought in the United States. J Hydrol Eng 18(7):737–745

Manzoni S, Vico G, Katul G, Palmroth S, Jackson RB, Porporato A (2013) Hydraulic limits on maximum plant transpiration and the emergence of the safety-efficiency trade-off. New Phytol 198(1):169–178

Martinez-Vilalta J, Poyatos R, Aguade D, Retana J, Mencuccini M (2014) A new look at water transport regulation in plants. New Phytol. doi:10.1111/nph.12912

McDowell N, Pockman WT, Allen CD, Breshears DD, Cobb N, Kolb T, Plaut J, Sperry J, West A, Williams DG, Yepez EA (2008) Mechanisms of plant survival and mortality during drought: why do some plants survive while others succumb to drought? New Phytol 178:719–739

McEwan RW, Dyer JM, Pederson N (2011) Multiple interacting ecosystem drivers: toward an encompassing hypothesis of oak forest dynamics across eastern North America. Ecography 34(2):244–256

Meinzer FC, Johnson DM, Lachenbruch B, McCulloh KA, Woodruff DR (2009) Xylem hydraulic safety margins in woody plants: coordination of stomatal control of xylem tension with hydraulic capacitance. Funct Ecol 23(5):922–930

Meinzer FC, Woodruff DR, Eissenstat DM, Lin HS, Adams TS, McCulloh KA (2013) Above- and belowground controls on water use by trees of different wood types in an eastern US deciduous forest. Tree Physiol 33(4):345–356

Meinzer FC, Woodruff DR, Marias DE, McColloh KA, Sevanto S (2014) Dynamics of leaf water relations components in co-occuring iso- and anisohydric conifer species. Plant Cell Environ 37:2577–2587

Novick KA, Oishi AC, Ward EJ, Siqueira MBS, Juang JY, Stoy PC (in press) Inter-annual variability in the biosphere-atmosphere exchange of CO_2 and H_2O in adjacent pine and hardwood forests: links to drought, rising CO_2, and seasonality

Nowacki GJ, Abrams MD (2008) The demise of fire and "mesophication" of forests in the eastern United States. Bioscience 58(2):123–138

O'Gorman PA, Schneider T (2009) The physical basis for increases in precipitation extremes in simulations of 21st-century climate change. Proc Natl Acad Sci USA 106(35):14773–14777

Oren R, Sperry JS, Katul GG, Pataki DE, Ewers BE, Phillips N, Schafer KVR (1999) Survey and synthesis of intra- and interspecific variation in stomatal sensitivity to vapour pressure deficit. Plant Cell Environ 22(12):1515–1526

Phillips NG, Ryan MG, Bond BJ, McDowell NG, Hinckley TM, Cermak J (2003) Reliance on stored water increases with tree size in three species in the Pacific Northwest. Tree Physiol 23(4):237–245

Plaut JA, Yepez EA, Hill J, Pangle R, Sperry JS, Pockman WT, McDowell NG (2012) Hydraulic limits preceding mortality in a pinon-juniper woodland under experimental drought. Plant Cell Environ 35:1601–1617

Quero JL, Sterck FJ, Martinez-Vilalta J, Villar R (2011) Water-use strategies of six co-existing Mediterranean woody species during a summer drought. Oecologia 166:45–57

Richter H (1997) Water relations of plants in the field: some comments on the measurement of selected parameters. J Exp Bot 87:1287–1299

Ritchie GA, Hinckley TM (1975) The pressure chamber as an instrument for ecological research. Adv Ecol Res 9:165–254

Schmid HP, Grimmond CSB, Cropley F, Offerle B, Su HB (2000) Measurements of CO_2 and energy fluxes over a mixed hardwood forest in the mid-western United States. Agric For Meteorol 103(4):357–374

Shifley S (2012) The Northern Forest Futures Project: examining past, present, and future trends affecting forests in and around the central hardwood forest regionq. In Miller GW, Schuler TM, Gottschalk KW, Brooks JR, Grushecky ST, Spong BD, Rentch JS (eds) 18th Central Hardwood Forest Conference, Morgantown, WV. US Department of Agriculture, Forest Service, Northern Research Station

Sperry JS (2000) Hydraulic constraints on plant gas exchange. Agric For Meteorol 104(1):13–23

Stoy PC, Katul GG, Siqueira MBS, Juang JY, Novick KA, McCarthy HR, Oishi AC, Oren R (2008) Role of vegetation in determining carbon sequestration along ecological succession in the southeastern United States. Glob Change Biol 14(6):1409–1427

Taneda H, Sperry JS (2008) A case-study of water transport in co-occurring ring- versus diffuse-porous trees: contrasts in water-status, conducting capacity, cavitation and vessel refilling. Tree Physiol 28(11):1641–1651

Thomsen JE, Bohrer G, Matheny AM, Ivanov VY, He LL, Renninger HJ, Schafer KVR (2013) Contrasting hydraulic strategies during dry soil conditions in *Quercus rubra* and *Acer rubrum* in a sandy site in Michigan. Forests 4(4):1106–1120

Turner NC, Long MJ (1980) Errors arising from rapid water loss in the measurement of leaf water potential by pressure chamber technique. Aust J Plant Physiol 7:527–637

Tyree MT, Sperry JS (1988) Do woody-plants operate near the point of catastrophic xylem dysfunction caused by dynamic water-stress—answers from a model. Plant Physiol 88(3):574–580

Van der Molen MK, Dolmana AJ, Ciais P, Eglinc T, Gobrond N, Lawe BE, Meirf P, Petersb W, Phillips OL, Reichsteinh M, Chena T, Dekkeri SC, Doubkov M, Friedl MA, Jungh M, van den Hurkl BJJM, de Jeua RAM, Kruijtm B, Ohtan T, Rebeli KT, Plummero S, Seneviratnep SI, Sitchg S, Teulingp AJ, van der Werfa GR, Wanga G (2011) Drought and ecosystem carbon cycling. Agric For Meteorol 151:765–773

Wang H, Schubert S, Koster R, Ham YG, Suarez M (2014) On the role of SST in the 2011 and 2012 extreme US heat and drought: a study in contrasts. J Hydrometeorol 15:1255–1273

Wayson CA, Randolph JC, Hanson PJ, Grimmond CSB, Schmid HP (2006) Comparison of soil respiration methods in a mid-latitude deciduous forest. Biogeochemistry 80(2):173–189

Wear DN, Greis JG (2012) In: Report GT (ed) The Southern Forest Futures Project: summary report. USDA Forest Service, Asheville, NC

Whitehead D, Edwards WRN, Jarvis PG (1984) Conducting sapwood area, foliage area, and permeability in mature trees of *Picea sitchensis* and *Pinus contorta*. Can J For Res-Rev Can Rech For 14(6):940–947